IOPscience iopscience.iop.org

Home Search Collections Journals About Contact us My IOPscience

Electron energy loss and X-ray absorption spectroscopy of rutile and anatase: a test of structural sensitivity

This article has been downloaded from IOPscience. Please scroll down to see the full text article.

1989 J. Phys.: Condens. Matter 1 797

(http://iopscience.iop.org/0953-8984/1/4/012)

View the table of contents for this issue, or go to the journal homepage for more

Download details:
IP Address: 171.66.16.90
The article was downloaded on 10/05/2010 at 17:05

Please note that terms and conditions apply.

J. Phys.: Condens. Matter **1** (1989) 797–812. Printed in the UK

Electron energy loss and x-ray absorption spectroscopy of rutile and anatase: a test of structural sensitivity

R Brydson†, H Sauer‡, W Engel‡, J M Thomas§, E Zeitler‡, N Kosugi‖ and H Kuroda‖

† Department of Physical Chemistry, University of Cambridge, Lensfield Road, Cambridge CB2 1EP, UK

‡ Fritz-Haber-Institut der Max-Planck-Gesellschaft, Faradayweg 4-6, D1000 Berlin 33 (Dahlem), Federal Republic of Germany

§ Davy–Faraday Laboratories, The Royal Institution, 21 Albemarle Street, London W1X 4BS, UK

‖ Department of Chemistry, Faculty of Science, University of Tokyo, Hongo, Tokyo 113, Japan

Received 15 July 1988

Abstract. The electron energy loss and x-ray absorption spectra of two phases of titanium dioxide—rutile and anatase— are reported. Although the nearest-neighbour environments of titanium and oxygen in both these structures are very similar, noticeable differences are observed between the electron energy loss and the x-ray absorption spectra. Attempts to model these differences using real-space multiple-scattering calculations are reasonably successful at the Ti K and O K edges. We propose an interpretation of the Ti $L_{2,3}$ edge, notably for the presence of a previously unobserved splitting on the L_3 edge.

1. Introduction

Titanium dioxide (TiO_2) forms three distinct polymorphs: rutile, anatase and brookite. This present study is concerned with the former two which offer a stringent test of the sensitivity of electron energy loss spectroscopy (EELS) and x-ray absorption spectroscopy (XAS) to subtle changes in the structure of a compound. In undertaking this test, we attempt to clarify the importance of short- and longer-range order in the interpretation of electron energy loss near-edge structure (ELNES) and x-ray absorption near-edge structure (XANES). This entails a comparison of our experimental findings with the projected densities of states (DOS) derived from various band-structure calculations of other workers, our real-space multiple-scattering calculations performed using the ICXANES computer code of [1], and the predictions of a number of previously published localised-cluster calculations. A similar, very stimulating investigation was performed in 1983 and was reported in [2]. Since that time, instrumentation has improved considerably, and consequently it seemed worthwhile to repeat the measurements with increased resolution and better signal statistics, especially with regard to the EELS measurements.

Under the conditions of small momentum transfer and small sample thickness the interpretation of ELNES follows along similar lines to that of XANES [3]. In the simple

0953-8984/89/040797 + 16 $02.50 © 1989 IOP Publishing Ltd

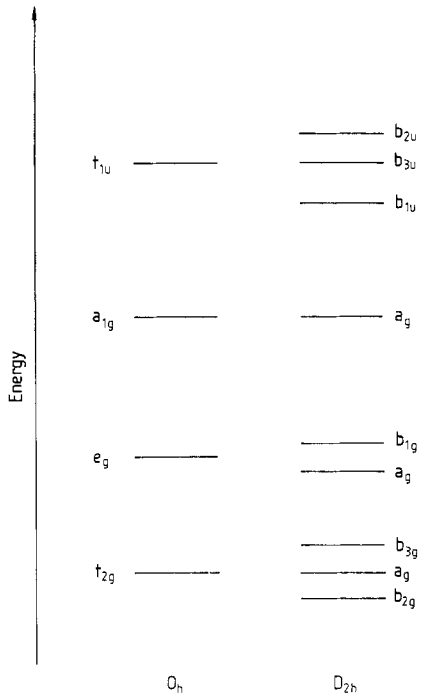

Figure 1. Schematic diagram of the lowest unoccupied MOs of a titanium atom surrounded by six oxygen nearest neighbours in octahedral O_h and orthorhombic D_{2h} symmetry.

single-electron picture, it can be shown that observed near-edge features reflect the symmetry-projected density of unoccupied states [4]. In reality, this may be modified by many-body effects, and the question arises to what extent many-electron effects have to be considered in order to explain the resultant near-edge structures.

Both rutile and anatase are tetragonal, rutile containing six atoms per unit cell and anatase twelve. In both structures, each titanium atom is coordinated to six oxygen atoms and each oxygen atom is coordinated to three titanium atoms. In each ease the coordination oxygen octahedron around the titanium atom is slightly distorted, two Ti–O distances being slightly greater (less than 0.1 Å) than the other four and some of or all the O–Ti–O bond angles deviating from 90°. This lowers the local point-group symmetry around the titanium atom from O_h to D_{2h} and D_{2d} in rutile and anatase, respectively. The essential difference between rutile and anatase lies in the secondary coordination [5] and in the way that the TiO_6 octahedra are joined together by sharing edges and corners. In rutile, two edges are shared and in anatase four.

Previous studies of TiO_2 have generally employed a symmetry-determined molecular orbital (MO) model as a starting point for the interpretation of both EELS and XAS spectra. If we consider a TiO_6^{8-} cluster consisting of a metal atom surrounded by oxygen nearest neighbours in orthorhombic D_{2h} symmetry (as for rutile), then we arrive at the MO energy level diagram shown in figure 1 (only the unoccupied levels are shown). The two lowest unoccupied orbitals containing mostly Ti 3d (but some O 2p) character separate into two groups: the threefold t_{2g} and the twofold e_g. These are known as the crystal-field orbitals and in perfect O_h symmetry they consist of two distinct levels, the lowering of symmetry to D_{2h} causing both of these to split as shown. Higher in energy come the a_{1g} and t_{1u} diffuse Ti—O anti-bonding orbitals, the t_{1u} being split in D_{2h} symmetry. In [6] a

self-consistent field X_α scattered wave cluster calculation for a TiO_6^{8-} cluster in perfect O_h symmetry was performed and values were derived for the splittings between the various MOs. The results show a t_{2g}–e_g splitting of 3.6 eV, the a_{1g} and t_{1u} lying 9.9 eV and 10.2 eV, respectively, above the t_{2g}.

Progressing from MO theory, in [2, 7] the band structure for rutile was calculated using the extended Hückel tight-binding method and it was compared with experimental EELS data. The DOS calculated exhibits two peaks in the conduction band (essentially band-broadened t_{2g} and e_g levels), their maxima separated by about 4.5 eV. Subsequently a similar calculation was performed for anatase [2], and a similar result was obtained except that the t_{2g} and e_g bands were found to be slightly closer (about 3.8 eV apart). More importantly the results show that the peaks in the DOS for each phase are at identical energies in both the titanium and the oxygen projections, suggesting that the local DOS around titanium and oxygen are essentially the same. This provides support for the MO picture and we shall return to this point later.

A further band structure of rutile [8], calculated using the linear combination of muffin-tin orbitals method, exhibits a splitting of about 2.5 eV between the centres of the t_{2g} and e_g bands. The DOS of all these calculations essentially show that the main character of the t_{2g} and e_g bands is Ti 3d with a small O 2p component in agreement with MO theory.

It is well known that, in some cases, band structures do not correlate with observed near-edge features. One of the most striking examples is the L_3/L_2 white-line intensity ratios in transition metals and their compounds, which is expected to be 2 : 1 by statistical arguments owing to the numbers of electrons in the $2p_{3/2}$ and $2p_{1/2}$ subshells. However, strong deviations from this ratio are found experimentally [9, 10] and it has been shown [11] that an atomic approach investigating excitations from $2p^63d^n$ to $2p^53d^{n+1}$ multiplet states is suitable for a theoretical explanation of the phenomenon. For these transitions a 2 : 1 ratio is only expected when the core hole spin–orbit interaction is much larger than the electrostatic direct and exchange interactions between the hole and the d electrons. In [12] the results of atomic multi-configuration Dirac–Fock calculations were reported for the excitation from 2p levels and good agreement was obtained between theory and experiment for the white-line ratios but, owing to solid state effects, which are neglected in the calculation, the detailed shape of their curves is often incorrect. In [13] the $M_{2,3}$ and $L_{2,3}$ absorption spectra for various transition-metal ions were calculated within the framework of ligand-field theory assuming an electric field of cubic symmetry. For $L_{2,3}$ excitations the spin–orbit interaction in the 2p shell is stronger than the other interactions so that the two components L_3 and L_2 are always well separated. Interactions between the 3d electrons, exchange interactions, as well as the 2p core hole–3d electron interaction give rise to abundant multiplet structure. The spin–orbit interaction in the 3d shell has been neglected. Their calculated spectra agree well with the measurements in [14] on 3d transition-metal fluorides, although it is clear that in some cases they have overestimated the covalency. Good agreement was also found with the results in [15] in which the multiplet structure of core p vacancy levels for 3d transition metal ions is calculated, with the inclusion of spin–orbit interactions but excluding the crystal-field effect. This suggests that in certain cases the effect of the crystal field is of little importance; however, as we shall discuss, this is not true for rutile and anatase. It is apparent from both these studies that the interaction between the 2p core hole and the 3d electrons is of great importance and, although calculations have not been performed on systems directly relevant to ours, we shall discuss the theoretical results in comparison with our experimental findings.

2. Instrumentation and preparation

The EELS microscope used in this present work has been described in detail elsewhere [16]. Briefly, it allows the parallel recording of energy loss electrons, improving the electron collection efficiency by approximately two orders of magnitude over serial detection systems used in previous studies. Moreover an energy resolution of 0.5 eV or less is routinely available. Together these two factors make it possible to obtain high-resolution spectra with extremely good statistics in a short period of time, thus minimising the problems of beam damage. The XAS measurements were made at the Photon Factory in the National Laboratory for High Energy Physics in Japan using beam line 7c which is equipped with an Si(111) crystal monochromator. The resolution is approximately 1 eV and the resultant spectra are considerably improved over previous measurements [2], especially in the pre-edge region. As regards sample preparation, anatase was obtained as a reagent-grade chemical powder, the rutile phase being prepared from this by heating for 6 h at 1100 °C. All samples were characterised before EELS and XAS analysis by powder x-ray diffraction, the EELS samples being then ground in a mortar and pestle and suspended in acetone or methanol and pipetted onto holey carbon grids. After acquisition of EELS spectra the sample area under study was characterised using electron diffraction. The EELS measurements were made on single crystals and it was observed that the near-edge structures were identical for crystals with different orientations of the *c* axis to the incident beam. This is important since rutile and anatase are anisotropic. The XAS measurements were made on polycrystalline samples and thus this problem was not encountered.

3. Spectra and theoretical calculations

In this section, we present our experimental EELS and XAS spectra together with our theoretical real-space multiple-scattering ICXANES calculations for both rutile and anatase. For each of the edge spectra, peak positions and, in some cases, widths are

Table 1. Positions of the various peaks in the EELS and XAS spectra of rutile labelled in figures 2, 4 and 6. All positions are relative to the first strong peak, the absolute energy loss of which is given at the bottom. The figures in square brackets denote the full width at half-maximum of the peaks in electronvolts. The numbers marked with an asterisk indicate that they have been derived by fitting the derivative of a peak with a Gaussian derivative to obtain a Gaussian fit. For an explanation of this procedure, see [31]. Errors in the Gaussian fitting procedure are difficult to assign, but it appears that these peak positions are accurate to about 0.1 eV. Absolute energy, Ti L_3 (peak A_3), 458.2 ± 0.2 eV; absolute energy, O K (peak A_3), 530.9 ± 0.2 eV; Ti L_3–L_2 separation (peak A_3 to peak A_3), 5.44 eV.

	Peak position relative to peak A_3 in rutile (eV)							
Edge	A_1	A_2	A_3	B_1	B_2	C_1	C_2	D_1
Ti K	−3.1	—	0	3.0		8.6	12.6	15.6
Ti L_3	−1.45	−0.81	0 [0.7]	1.97	2.86	—	—	—
				1.9 [0.9]*	2.9 [0.9]*			
Ti L_2	—	—	0 [1.6]	2.45 [2.3]		—	—	—
				2.0 [1.2]*	2.8 [1.4]*			
O K	—	—	0 [1.8]	2.58 [2.3]		9.0	11.6	14.0

Table 2. Positions of the various peaks in the EELS and XAS spectra of anatase labelled in figures 3, 5 and 7. The nomenclature is as for table 1. Absolute energy, Ti L_3 (peak A_3), 458.2 ± 0.2 eV; absolute energy, O K (peak A_3), 531.1 ± 0.2 eV; Ti L_3–L_2 separation (peak A_3 to peak A_3), 5.44 eV.

	Peak position relative to peak A_3 in anatase eV							
Edge	A_1	A_2	A_3	B_1	B_2	C_1	C_2	D_1
Ti K	−3.2	−1.3	0	2.3		7.5	11.1	15.9
Ti L_3	−1.53	−0.87	0 [0.7]	1.77	2.45	—	—	—
				1.8 [0.8]*	2.8 [1.0]*			
Ti L_2	—	—	0 [1.5]	1.97 [2.3]		—	—	—
				2.0 [1.2]*	2.8 [1.6]*			
O K	—	—	0 [1.8]	2.58 [2.3]		8.0	—	13.5

given for reference purposes in tables 1 and 2; they include the Ti K edge data measured using XAS together with the EELS data for the Ti $L_{2,3}$ and O K edges. All experimental EELS spectra have been deconvoluted so as to remove multiple scattering using the Fourier ratio method [3, 17]. While this has little effect on the Ti $L_{2,3}$ edges, a small change was apparent in the ELNES of the O K edges. We also compare our results with the theoretical calculations of others.

In figures 2 and 3 (upper curves), we present the XAS Ti K edge spectra of rutile and anatase, respectively. The absolute energies have been set so as to match the data in [2];

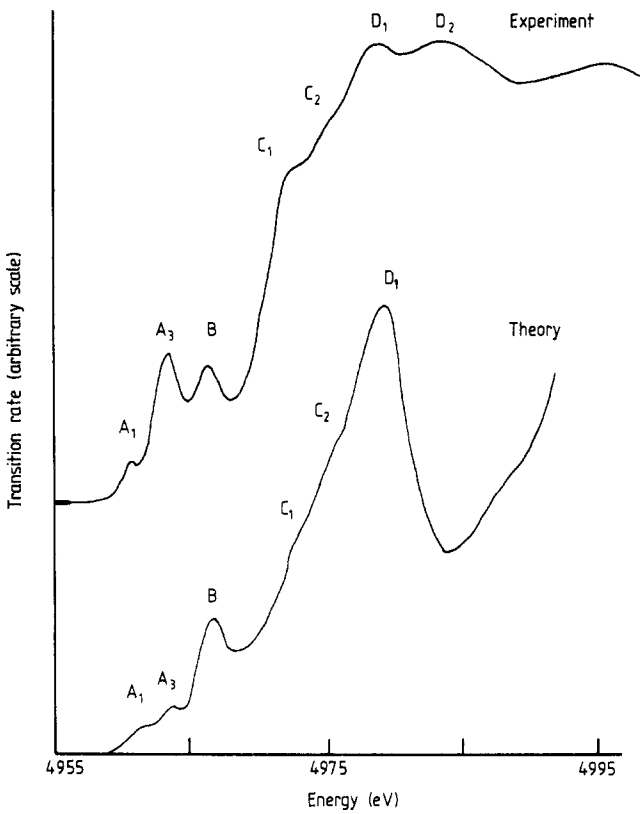

Figure 2. The experimental XAS Ti K edge of rutile (curve labelled Experiment). The peak positions are given in table 1. The results (curve labelled Theory) of our ICXANES calculations for the Ti K edge in rutile. Five shells of atoms have been included together with a damping of −0.5 eV. Features corresponding to the peaks labelled in the experimental spectrum have been indicated; further details are given in the text.

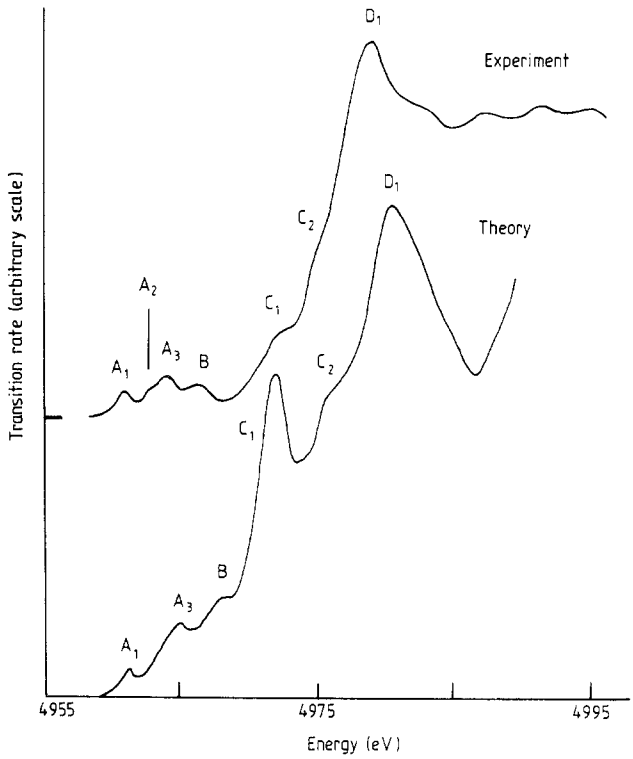

Figure 3. The experimental XAS Ti K edge of anatase (curve labelled Experiment). The peak positions are given in table 2. The results (curve labelled Experiment) of our ICXANES calculations for the Ti K edge in anatase. Five shells of atoms have been included together with a damping of −0.5 eV. Features corresponding to the peaks labelled in the experimental spectrum have been indicated; further details are given in the text.

however, it should be noted that there is some disagreement in the value of the absolute edge energies found by the various experimentalists. In the Ti K edge spectrum of rutile (figure 2), we have labelled an extra feature C_2 which is only weakly visible on the steeply rising shoulder; this is also present in the spectra in [18, 19]. Considering the dipole approximation appropriate to XAS and EELS, K edges essentially involve transitions from the 1s core level to p-like states around the atom. Using the predictions of simple MO theory together with the results of a band-structure calculation and comparison with experimental EELS results, in [2] the peaks in the spectra were assigned in terms of transitions to MOs. For both rutile and anatase, peaks A_3 and B were assigned to the t_{2g} and e_g final states assuming quadrupolar transitions ($1s \rightarrow 3d$) following the work in [20, 21] and elsewhere. Peaks C_1 and C_2 in anatase and rutile are assigned to $1s \rightarrow 4p$ transitions with a simultaneous shakedown creating a hole in the highest occupied ligand orbitals following the work in [22]. Peaks D_1 in rutile and anatase are explained as transitions to the t_{1u} level (see figure 1). This leaves the weak peak A_1 present in both rutile and anatase which in [2] was assigned to an excitonic transition within the forbidden band gap (Frenkel core exciton). The weak feature A_2 arrowed in figure 3 (upper curve) is only visible in anatase and has not been observed by others; this is presumably due to our superior energy resolution.

We now consider our ICXANES results. For this and all subsequent ICXANES calculations for rutile and anatase, phase shifts and matrix elements were obtained by imposing a muffin-tin potential on the structure in question [23]. The muffin-tin radii were chosen to be equal to the ionic radii of Ti^{4+} and O^{2-}, i.e. $r(\mathrm{Ti}) = 1.29$ au and $r(\mathrm{O}) = 2.49$ au (other values were investigated, notably the prescription given in [24], but apart

from the O K edge there was little variation in the final ICXANES results). The exchange parameter α was taken to be 0.8. Owing to the arbitrary position of the muffin-tin energy zero, these and all other theoretical curves have been aligned to experiment in such a way that the first peaks coincide. We have included five shells around the central titanium atom corresponding to a cluster radius of approximately 10 au (50 atoms), together with a damping of -0.5 eV. The shells were chosen so as to be roughly 1 au apart in space. We have not taken account of any core hole effects (this may be done by use of an excited-atom potential for the absorber [25]—but in this case it did not produce any significant differences).

In figures 2 and 3 (lower curves), we show the results of our ICXANES calculations for the Ti K edges in rutile and anatase, respectively. As can be seen for rutile (figure 2), our calculated curve models the major features A_1, A_3, B, C_1 and D_1 reasonably well. Peak D_2 is notably absent in our calculated curve and the shoulder C_2 is only weakly visible. The agreement is also good for anatase (figure 3) where the theory correctly reproduces peaks A_1, A_3, B, C_1, C_2 and D_1, the structure further out from the edge again tending to deviate from experiment. Since the ICXANES program calculates only the rate of dipolar transitions, the good agreement between the calculated spectra and the experimental data indicates that all the peaks A_1–D_1 represent transitions to states having at least a significant amount of p symmetry. Moreover peak A_1 is present in the calculated spectra even though core hole effects have been neglected. The assignment of A_1 to an excitonic transition as has been done in [2] and elsewhere on the results of band-structure calculations therefore appears to be rather questionable.

Even in very early investigations the weak pre-edge structures at transition-metal K edges were related to empty 3d orbitals [26] and, since the work in [20, 21, 27] and elsewhere, it seems that there is a general consensus in assigning peaks A_3 and B to quadrupolar transitions to t_{2g} and e_g orbitals. Our ICXANES results suggest that a significant 3d–4p orbital mixing occurs in rutile and anatase, forming t_{2g} and e_g bands which do not possess solely d symmetry. Thus, dipolar transitions into these bands can occur. This interpretation is supported by the recent experimental results in [28] in which the Ti K edges of various minerals were measured. In all investigated samples, titanium is surrounded by six oxygen atoms in a more or less distorted octahedron. A correlation was found between the intensity of the pre-edge structure and the bond angle variance in silicates and some oxides which should give rise to increased 3d–4p orbital mixing. Furthermore, in [28], it was observed that the presence of three pre-edge features at the Ti K edge (A_1, A_3 and B) is accompanied by an increase in distortion at the titanium site. The ICXANES calculations also predict the presence of peaks C_1 and C_2 in both polymorphs despite the fact that it is based on single-electron theory and hence neglects many-electron effects. Therefore the explanation in [2] that these are in fact $1s \rightarrow 4p$ shakedown transitions is seemingly refuted by our calculations. In terms of MO theory, we may assign the peaks C_1 and C_2 in anatase and rutile to transitions to the t_{1u} orbitals (note the $1s \rightarrow a_{1g}$ is dipole forbidden) in rough agreement with the MO calculation in [6]. The peaks D_1 and D_2, meanwhile, must be due to higher-lying t_{1u}-type orbitals ($1s \rightarrow$ p transitions) as assigned by Poumellec in [19].

The success in modelling the XANES of the Ti K edges in rutile and anatase demonstrates that the multiple-scattering approach using a muffin-tin form for the potential of each atom is adequate. One-electron theory is able to account for the main features of the Ti K edges, any discrepancies being probably due to many-electron effects (see, e.g., [29]). The theory reveals slight differences in the XANES of the two polymorphs which must arise from the outer-lying shells since the first-nearest-neighbour shells are

almost identical. Thus long-range effects play an important role in determining the resultant near-edge structure and must be taken into account in order to model the Ti K edges satisfactorily.

For $L_{2,3}$ edges, transitions to the lowest states of the conduction band take place; these are mainly formed from Ti 3d and O 2p orbitals. Since the 3d electrons are relatively tightly bound and the d band is quite narrow, it is believed that an atomic (short-range) approach is suitable for describing the $L_{2,3}$ edges in transition metals [12]. Thus, bearing in mind the similarity of the first coordination shells in the two polymorphs, one would expect to see little or no difference between the resultant $L_{2,3}$ spectra.

In figures 4 and 5 (upper curves), we present the EELS Ti $L_{2,3}$ edges for rutile and anatase, respectively. The energy resolution for these spectra is approximately 0.3 eV. The most obvious feature of the Ti $L_{2,3}$ edges is the spin–orbit splitting of the L_3 and L_2 lines; this is 5.4 eV in both rutile and anatase. Furthermore, the L_3 line and the L_2 line for both phases are initially split into two (A_3 and B) as observed using XAS in [20] and using EELS in [7]; in both papers, this is attributed to the crystal-field splitting of the t_{2g} and e_g orbitals. We, however, observe a further splitting on the second peak (B) of the L_3 edge (B_1 and B_2), which appears as a low-energy shoulder for rutile and a high-energy shoulder for anatase. This feature was also observed in earlier EELS measurements on a

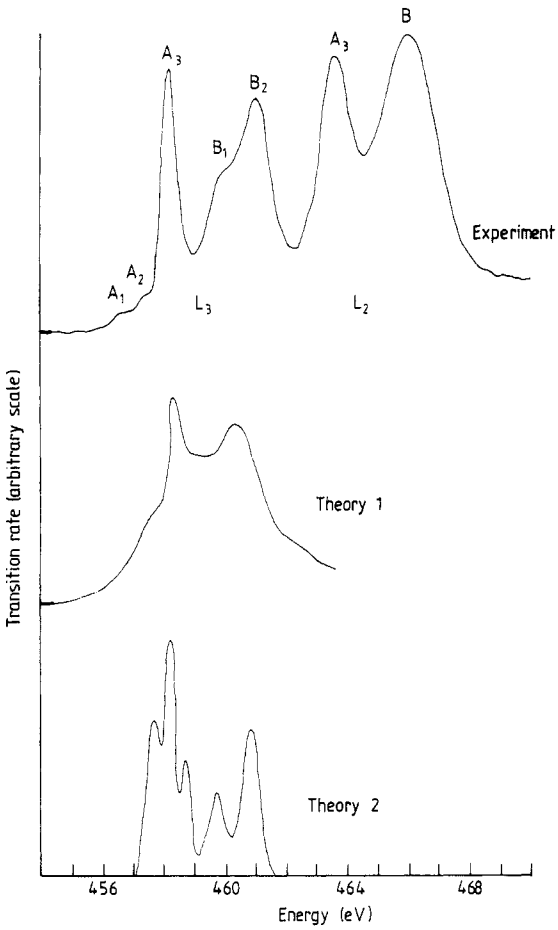

Figure 4. The experimental EELS spectrum (labelled Experiment) of the Ti $L_{2,3}$ edge in rutile after background subtraction and deconvolution. The peak positions are given in table 1. The results (curve labelled Theory 1) of our ICXANES calculations for the Ti L_3 edge in rutile. Five shells of atoms have been included together with a damping of -0.5 eV. Further details are given in the text. The conduction band DOS (curve labelled Theory 2) for VO_2 (rutile) taken from [39].

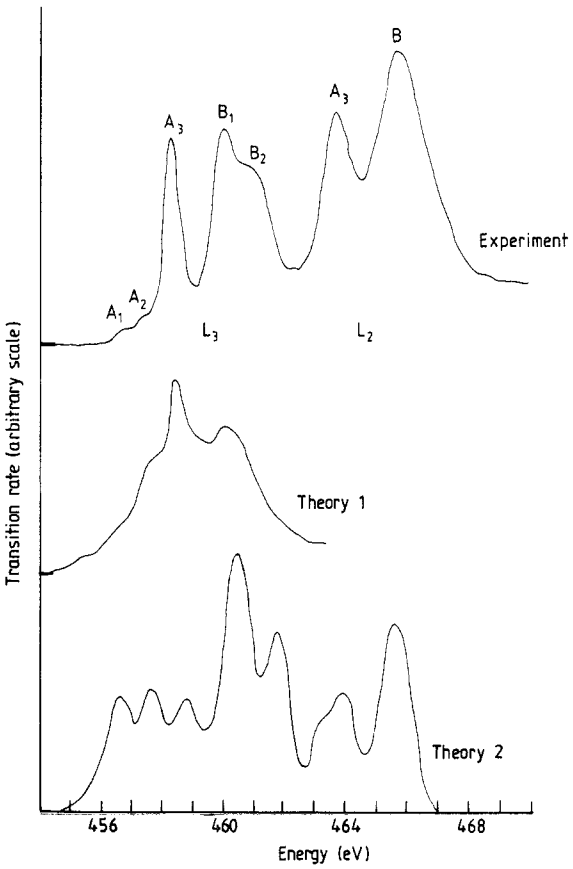

Figure 5. The experimental EELS spectrum (labelled Experiment) of the Ti $L_{2,3}$ edge in anatase after background subtraction and deconvolution. The peak positions are given in table 2. The results (curve labelled Theory 1) of our ICXANES calculations for the Ti L_3 edge in anatase. Five shells of atoms have been included together with a damping of −0.5 eV. Further details are given in the text. The theoretical $L_{2,3}$ edge of Ti^{3+} (curve labelled Theory 2) calculated in [13] assuming a localised transition-metal ligand cluster. See text for explanation.

titania sol which consisted of a mixture of rutile and anatase [30]. Closer examination of the Ti L_3 edges reveals the presence of two weak peaks (A_1 and A_2) prior to the first intense peak A_3. These are present in the spectra of both phases and were not observed in the results of the sol [30].

There are significant differences between the Ti L_3 spectra for rutile and anatase, notably in the relative intensities of peaks B_1 and B_2. A fit of Gaussians [31] to the L_3 structures of rutile and anatase shows, however, that, within experimental error, peak positions and widths are almost identical for both polymorphs (see tables 1 and 2), indicating that the long-range order is of little importance. Furthermore, we have reported that our measured and derived linewidths are in good agreement with x-ray photo-electron spectroscopy data [30, 32].

The L_2 edges of rutile and anatase exhibit differing energy spacings between peaks A_3 and B. This may be easily explained if we assume that the L_2 structure is simply a broadened version of the L_3 edge, owing to the increased Coster–Kronig decay channel. Thus the splitting of the second peak B is concealed and the effect is then due to the relative intensities of the two peaks which actually compose this broadened peak. In rutile the higher-energy peak is stronger as can be seen from the L_3 edge (B_1 and B_2) and thus shifts the resultant composite peak to higher energy loss, compared with anatase where the lower-energy peak is of greater intensity. We are able to decompose the broad peak B successfully into the sum of two Gaussians split by roughly the same amount as

noted in table 1 and 2. This suggests in terms of a MO picture that the crystal-field splittings of the two polymorphs are the same, contradicting the results obtained in [2], which is to be expected since the distances in the first coordination shell are very similar.

In figures 4 and 5 (lower curves), we show the results of our ICXANES calculations. The parameters for the muffin-tin potential construction and the multiple-scattering calculation are the same as for the Ti K edge. We have not included core hole effects as suggested by some workers [33, 34] since in practice this produced little difference form the final result (also, for MgO, we found this unnecessary in order to model the $L_{2,3}$ edge [35]. The major problem with modelling $L_{2,3}$ edges is that the ICXANES theory assumes that, in a transition from an initial state of angular momentum l, there is no interference between the channels $l+1$ and $l-1$. For $L_{2,3}$ edges, this corresponds to the $p \rightarrow d$ and $p \rightarrow s$ transitions. The matrix elements governing the $\Delta l = -1$ transitions are much smaller than those of the $\Delta l = +1$ and thus the contribution of the former is usually negligible (as was found to be the case here); however, interference effects could produce deviations from this. In [33], it was stated that in polycrystalline samples any cross terms due to interference effects disappear; our EELS measurements were made on single crystals and, as stated, we observed no change in edge structure for different crystal orientations. Therefore, at present, we have to ignore this point and simply view the $L_{2,3}$ edge as essentially reflecting the Ti 2p–3d transitions. Since the ICXANES theory does not include the effects of spin–orbit splitting of the initial state, we have simply matched the ICXANES results with the L_3 edge in both cases (the L_2 edge being simply a broadened version of the L_3 edge in the single-electron approximation). As can be seen, they predict, in both phases, a sharp t_{2g} peak separated by approximately 2 eV from a relatively broad e_g peak. However, no splitting is apparent on the e_g peak in either of the theoretical curves. This is in qualitative agreement with the results of band theory [2, 8], which is to be expected since the ICXANES method is formally equivalent to a Korringa–Kohn–Rostocker (KKR) band-structure calculation. We did investigate the results of ICXANES calculations for one shell of oxygen atoms surrounding a central titanium atom and subsequently found that the main structure of the t_{2g} and e_g peaks was reproduced. This suggests that the $L_{2,3}$ edge is essentially reflecting the nearest-neighbour environment, a point which we shall return to in our discussion of an atomic interpretation. If we progressively distorted the two axial bonds in the single shell, then for large distortions (about 0.3 Å) it was possible to produce a broader e_g peak, but nothing that matched satisfactorily with experiment. The ICXANES results suggest some tailing on the low-energy side of the initial peak A_3, but little that could explain the presence of the weak peaks A_1 and A_2. Of course, these could be due to excitonic transitions below the band gap, in which case the ICXANES approach would not be expected to predict this but, when the previous analysis of the Ti K edges is borne in mind, it is all too easy to assign any weak pre-peaks as excitons when we have in fact no decisive proof. It is notable that a peak similar to peak A_1 has been observed in the Ti $L_{2,3}$ edge of TiS_2 measured using XAS [36] and we believe that these could be due to spin-forbidden transitions, as we shall discuss later.

We now concern ourselves with an explanation for the splitting of peak B on the L_3 edges. In terms of an MO picture, this splitting represents a splitting of the e_g band. The band-structure calculations presented for rutile and anatase [2, 8] show no sign of this. They do exhibit a broad e_g band; however, no splitting is discernible. The MO model does predict splitting of both the t_{2g} and the e_g bands in the case of a lowering of symmetry from O_h to D_{2h}, the splitting of the e_g being expected to be greater than that of the t_{2g} [37]. In [7], it was concluded that the distortion in rutile will affect the resulting orbital

energies by less than 0.1 eV compared with those of a perfect octahedron. However, paramagnetic resonance measurements on V^{4+} ions substituted in TiO_2 [38] suggest larger splittings. VO_2 has a rutile structure above 341 K [39] with slightly less distortion than in rutile. In [39] an augmented plane-wave calculation of the band structure was performed; the conduction band DOS of this exhibits considerable structure which is shown in figure 4 (lower curve) compared with the Ti L_3 edge in rutile. As can be seen, the t_{2g} manifold is split into three components (as would be expected from MO theory (see figure 1) although the splitting is small. The e_g manifold, however, reveals two peaks separated by about 1 eV, the lower-energy peak being about half the size of the higher-energy peak. This is in excellent agreement with our experimental Ti L_3 edge for rutile. Further evidence for the presence of ground-state splitting is evident in the Ti K edge spectrum for tetragonal $BaTiO_3$ [18]. Titanium in $BaTiO_3$ is octahedrally coordinated to oxygen as in rutile; however, the distortions are greater than in rutile [5] and the Ti K edge exhibits a broad e_g peak which shows a splitting of roughly 2 eV. Moreover, in [40], it was shown that small distortions of the absorbing atom environment result in a broadening or splitting of features in the Fe and Co K edges of various oxides.

As we have discussed before [30], another possible explanation for the size of the splitting arises from the possibility of a dynamic Jahn–Teller effect [41]. Optical measurements on Ti^{3+} ions in solution [42], and incorporated into a variety of systems, notably Al_2O_3 [43, 44], indicate a splitting of the e_g doublet. This has been attributed to a coupling of the electronic and vibrational states, commonly known as the dynamic Jahn–Teller effect. A similar splitting occurs in the t_{2g} levels but for octahedrally coordinated transition metals this is considerably smaller [37]. Admittedly in optical measurements the excited-state configuration is different from that in our EELS experiment (an electron in the e_g orbitals and a hole in the t_{2g} orbitals compared with an electron in the e_g orbitals and a hole in the 2p shell). Also the crystal field and the strength of the Jahn–Teller coupling may be different. However, it is useful to compare our results with those obtained using optical methods. The t_{2g} to highest e_g orbital transition energies for $Al_2O_3:Ti^{3+}$ and Ti^{3+}(aq) are 2.4 eV and 2.5 eV, respectively. Since the Ti–O bond distance in both forms of TiO_2 is slightly shorter than in Ti^{3+}(aq), we may estimate the crystal-field splitting to be 2.7–2.9 eV in Ti^{4+} (in agreement with the EELS values in tables 1 and 2). At 300 K the e_g splitting in these two systems is 0.31 eV and 0.36 eV, respectively; however, this increases with increasing temperature. Unfortunately the temperature of the specimen in our EELS experiment is unknown but is probably quite high owing to intense irradiation with 60 keV electrons. For the $Al_2O_3:Ti^{3+}$ system the e_g splitting is expected to increase to 0.51 eV at 1000 K [44]. This is still smaller than our result but this may be due to the differences between the two systems.

As stated, an atomic approach is often more successful than a band-structure approach in the interpretation of near-edge structures especially for the L edges of transition metals and their compounds. From the spectra in figures 4 and 5 (upper curves), we deduce an L_3 to L_2 white-line intensity ratio of about 0.7 for both rutile and anatase, obtained by subtracting a contribution from the steadily increasing edge background (representing transitions to the continuum) and measuring the area under each edge. This is far from the theoretical ratio of 2 to 1 expected from statistical arguments, suggesting that single-electron theory is not sufficient to explain our results. In [15] the multiplet structure core 2p vacancy levels for Ti^+, Ti^{2+} and Ti^{3+} were calculated assuming them to be free ions. It is difficult to assign a particular ionic charge to transition-metal ion in a complex, owing to the covalency. However, none of the calculated spectra for titanium ions matches well with our spectra, suggesting in this case that the crystal-

field effect, which was ignored in [15], is important. The atomic multi-configuration Dirac–Fock calculations in [12] also ignore solid state effects. That calculation for Ti^{4+} shows three peaks centred at around 456, 460 and 466 eV, the latter two being approximately five times as large as the first. It is stated that these arise from $p_{3/2} \rightarrow d_{3/2}$, $p_{3/2} \rightarrow d_{5/2}$ and $p_{1/2} \rightarrow d_{3/2}$ transitions, respectively. An L_3 to L_2 white-line intensity ratio of 0.91 was predicted for Ti^{4+} which is in reasonable agreement with our measured values. These results show that the spin–orbit interaction of the 3d electron cannot be neglected. Solid state effects, such as the presence of the crystal field, would be expected to cause further splitting. This could perhaps explain the presence of the two weak initial peaks A_1 and A_2 (see figures 4 and 5) present on the Ti L_3 edge in both rutile and anatase. Because these peaks are so weak, it seems probable that they arise from the spin-forbidden $p_{3/2} \rightarrow d_{3/2}$ transition. Comparison of our measured $L_{2,3}$ spectra with the calculated spectra in [13] may also be made. The theoretical $L_{2,3}$ spectrum in [13] for Sc^{3+}, which has the same configuration as Ti^{4+}, exhibits two main lines at each of the L_3 and L_2 edges which are split as a result of the crystal field. There are some further structures which could correspond to peaks A_1 and A_2 and the splitting of peak B, but these are very weak and are hidden on convolution with a broadening function. The theoretical curve from [13] for Ti^{3+} is considerably more complicated and is shown in figure 5 (lower curve) compared with the Ti L_3 spectrum of anatase. As can be seen, the theoretical curve (calculated with a resolution of 1 eV and a crystal-field splitting of 2.52 eV) exhibits peaks in close correspondence to our experimental results; the intensities, however, are different, notably the first strong peak A_3 (furthermore the L_3 to L_2 ratio is obviously incorrect). This might be due to the differences between the two systems, but from the results for Sc^{3+} and Ti^{3+} the main cause of any multiplet structure seems to be as a result of 2p core hole–3d electron and d–d electron interactions. The

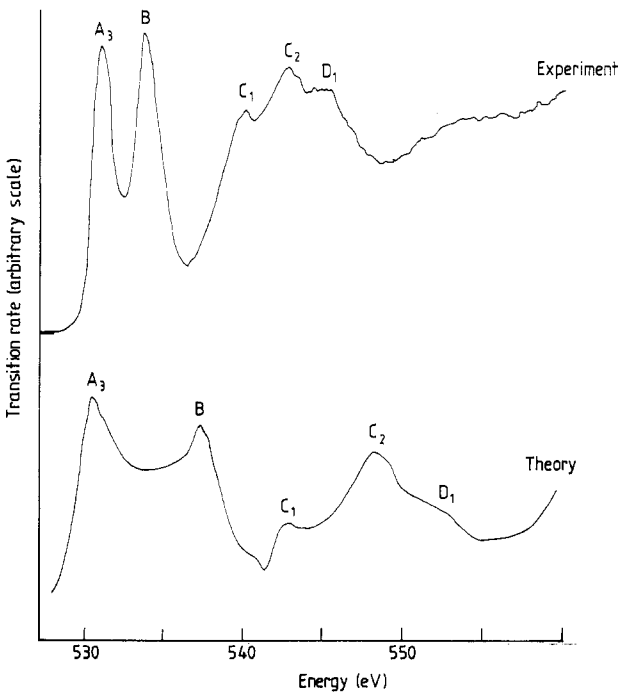

Figure 6. The experimental EELS spectrum (labelled Experiment) of the O K edge in rutile after background subtraction and deconvolution. The peak positions are given in table 1. The results (curve labelled Theory) of our ICXANES calculations for the O K edge in rutile. Six shells of atoms have been included together with a damping of −0.5 eV. Features corresponding to the peaks labelled in the experimental spectrum have been indicated; further details are given in the text.

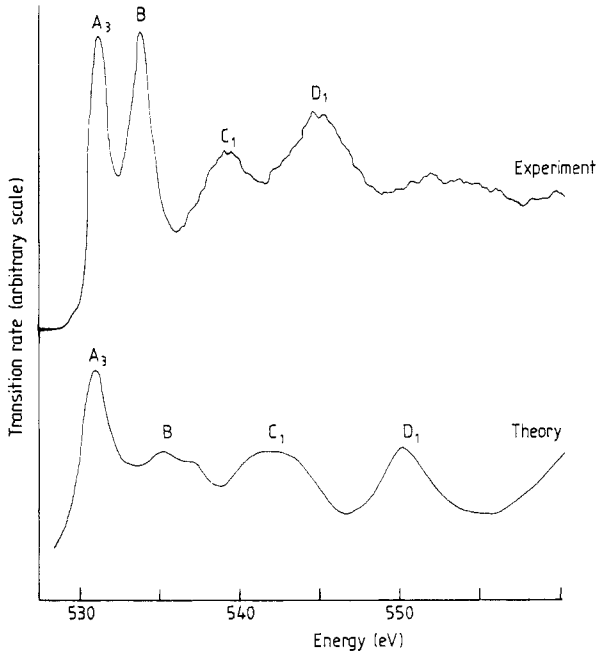

Figure 7. The experimental EELS spectrum (labelled Experiment) of the O K edge in anatase after background subtraction and deconvolution. The peak positions are given in table 2. The results (curve labelled Theory) of our ICXANES calculations for the O K edge in anatase. Six shells of atoms have been included together with a damping of −0.5 eV. Features corresponding to the peaks labelled in the experimental spectrum have been indicated; further details are given in the text.

qualitative agreement in figure 5 together with the correctly predicted L_3 to L_2 intensity ratio in [12] tend to support the quasi-atomic multiplet structure explanation for the detailed shape at the Ti $L_{2,3}$ edge. However, our results suggest that the $L_{2,3}$ edge cannot be solely viewed in terms of a localised atomic cluster. If this was so, then we would see no difference between rutile and anatase, which we clearly do, since the nearest-neighbour environments of the titanium atom are almost identical in both phases. Clearly the effect of the p–d and d–d interactions is important but this must be modified by the crystal field and further longer-range effects.

Finally we present in figures 6 and 7 (upper curves) our experimental EELS O K edge spectra for rutile and anatase recorded with an energy resolution of about 0.5 eV. As can be seen, there do exist differences chiefly in the peaks lying 8–15 eV from the edge. Both edges exhibit two initial peaks A_3 and B, which in [7] were assigned as transitions to the t_{2g} and e_g bands, respectively. Unlike the Ti L_3 edge the e_g band is not split although it is slightly broader (see tables 1 and 2). This suggests that the splitting is specific to the titanium, adding weight to the quasi-atomic transition viewpoint for the transition-metal $L_{2,3}$ structure. At higher energy losses, rutile exhibits three peaks C_1, C_2 and D_1 while anatase shows only two peaks C_1 and D_1. The EELS O K edge spectrum in [7] has a significantly worse signal-to-noise ratio (owing to serial recording of the spectrum) and the peaks C_2 and D_1 were not resolved. The peak positions are in rough agreement with those on the Ti K edges of the respective phases and thus we may assign the peaks C_1 and C_2 in rutile and C_1 in anatase to the lowest unoccupied t_{1u} final states. The peaks D_1, meanwhile, constitute transitions to higher-lying t_{1u} type orbitals.

In figures 6 and 7 (lower curves), we show the results of our ICXANES calculations for a cluster consisting of six shells (of radius approximately 10 au, i.e. 50 atoms) surrounding a central oxygen atom together with a damping of 0.5 eV. To model the effect of the

core hole, we have employed the $(Z + 1)^*$ approximation [25] in which the central atom is replaced by the $Z + 1$ element in an excited configuration in the muffin-tin potential calculation. The inclusion of this, however, produced very little difference from the results obtained from ground-state calculations. First, it should be noted that the agreement is poor when we consider the positions of the various peaks. The gross features and relative intensities, however, are reproduced quite well, the ICXANES results correctly predicting the presence of three peaks C_1, C_2 and D_1 in rutile and only two C_1 and D_1 in anatase in the extended O K edge structure. In both cases, we note that, if we displace the theoretical curve so that the second peaks coincide, then we achieve better agreement in the higher-energy-loss peaks. This effect has been noted before and could possibly be due to the energy dependence of the potentials, notably the energy-dependent exchange correlation between the excited electron and the valence electrons [29]. Indeed some researchers suggest artificially compressing the energy scales so as to match experiment and theory [2, 29]. The results of our calculations do show, however, that full multiple-scattering one-electron theory adequately describes the O K edges in both polymorphs and that it is necessary to consider the longer-range order if we want to model successfully the differences in the measured spectra.

4. Conclusions

This study has revealed that EELS, conducted in an electron microscope with the combined facilities of a parallel detection system and good energy resolution, constitutes a very sensitive probe of the solid state which may be used as a complementary technique to XAS. Although the two phases of TiO_2, rutile and anatase, possess very similar short-range titanium and oxygen environments, both EELS and XAS are able to detect significant differences in all the various edge structures. While these suggest that qualitatively the energy separations of the electronic levels of the unoccupied DOS are reasonably similar, the transition strengths may differ markedly between the two phases. Furthermore, we are able to model these differences reasonably well at the Ti K and O K edges using real-space multiple-scattering calculations and these results emphasise the importance of long-range order in determining the observed structure. This approach fails, however, at the Ti $L_{2,3}$ edge where we are unable to model a previously unobserved splitting at the L_3 edge. Since the ICXANES approach is formally equivalent to a KKR band-structure calculation, it is not surprising that the computed band structures of rutile and anatase also do not predict this feature. We discuss possible explanations of this splitting involving both ground-state and dynamic Jahn–Teller effects; however, the well known failure of band theory to explain the anomalous L_3 to L_2 white-line ratios suggests that we must view the L edges of the 3d transition metals and compounds from a quasi-atomic viewpoint. We compare our results with the theoretical localised-cluster calculations of others and find qualitative agreement especially with the work in [13]. While at this stage we do not have conclusive proof, we feel that the latter explanation is in fact the true one. This is not the whole story, however, since if this were the sole explanation then it would be thought that there would little or no difference between the Ti $L_{2,3}$ edges of rutile and anatase, when in fact there exists a difference in relative intensities. Thus there must exist some longer-range influence as well, which modifies the quasi-atomic multiplet structure produced by the short-range environment.

Acknowledgments

We would like to express our gratitude to Dr D D Vvedensky for his invaluable advice and to Beiping Luo for developing the data-processing programs. We also acknowledge with thanks support from the Science and Engineering Research Council (for a studentship to RB) and are grateful to the Max-Planck-Gesellschaft and the Japanese Research and Development Corporation for catalysing collaboration between the authors.

References

[1] Vvedensky D D, Saldin D K and Pendry J B 1986 *Comput. Phys. Commun.* **40** 421
[2] Grunes L A 1983 *Phys. Rev.* B **27** 2111
[3] Egerton R F 1986 *Electron Energy Loss Spectroscopy in the Electron Microscope* (New York: Plenum)
[4] Azaroff L V and Pease D M 1974 *X-ray Spectroscopy* ed. L V Azaroff (New York: McGraw-Hill)
[5] Wyckoff R W G 1960 *Crystal Structures* vol 1 (New York: Wiley–Interscience)
[6] Tossell J A, Vaughan D J and Johnson K H 1974 *Am. Mineral.* **59** 319
[7] Grunes L A, Leapman R D, Wilker C N, Hoffman R and Kunz A B 1982 *Phys. Rev.* B **25** 7157
[8] Kasowski R V and Tait R H 1979 *Phys. Rev.* B **20** 5168
[9] Leapman R D and Grunes L A 1980 *Phys. Rev. Lett.* **45** 397
[10] Leapman R D, Grunes L A and Fejes P L 1982 *Phys. Rev.* B **26** 614
[11] Barth J, Gerken F and Kunz C 1983 *Phys. Rev.* B **28** 3608
[12] Waddington W G, Rez P, Grant I P and Humphreys C J 1986 *Phys. Rev.* B **34** 1467
[13] Yamaguchi T, Shibuya S, Suga S and Shin S 1982 *J. Phys. C: Solid State Phys.* **15** 2641
[14] Nakai S, Ogata K, Ohashi M, Sugiura C, Mituishi T and Maezawa H 1985 *J. Phys. Soc. Japan* **54** 4034
[15] Gupta R P and Sen S K 1975 *Phys. Rev.* B **12** 15
[16] Engel W, Sauer H, Brydson R, Williams B G, Zeitler E and Thomas J M 1988 *J. Chem. Soc. Faraday Trans.* I **84** 617
[17] Egerton R F 1976 *Solid State Commun.* **19** 737
[18] Balzarotti A, Comin F, Incoccia L, Piacentini M, Mobilio S and Savoia A 1980 *Solid State Commun.* **35** 145
[19] Poumellec B, Marucco J F and Touzelin B 1987 *Phys. Rev.* B **35** 2284
[20] Fisher D W 1970 *J. Appl. Phys.* **41** 3561 1972 *Phys. Rev.* B **5** 4219
[21] Albrecht G 1966 *Rontgenspectren und Chemische Bindung* (Leipzig: Karl Marx University) p 3
[22] Bair R A and Goddard W A 1980 *Phys. Rev.* B **22** 2767
[23] Loucks T L 1967 *Augmented Plane Wave Method* (New York: Benjamin)
Mattheiss L F 1964 *Phys. Rev.* A **133** 1399
[24] Norman D, Garg K B and Durham P J 1985 *Solid State Commun.* **56** 895
[25] Brydson R, Vvedensky D D, Engel W, Sauer H, Williams B G, Zeitler E and Thomas J M 1988 *J. Phys. Chem.* **92** 962
[26] Borovsky I B 1940 *C. R. (Dokl.) Acad. Sci. URSS* **26** 764
[27] Wainstein E J, Shurakowski E A and Stari I B 1959 *Z. Neorgan. Khim.* **4** 245
[28] Waychunas G A 1986 *J. Physique Coll.* C8 841
[29] Davoli I, Marcelli A, Bianconi A, Tomellini M and Fanfoni M 1986 *Phys. Rev.* B **33** 2979
[30] Brydson R, Williams B G, Engel W, Sauer H, Zeitler E and Thomas J M 1987 *Solid State Commun.* **64** 609
[31] Brydson R, Williams B G, Saver H, Engel W, Schlögl R, Muhler M, Zeitler E and Thomas J M 1988 *J. Chem. Soc. Faraday Trans.* I **84** 631
[32] Fuggle J C and Alvarado S F 1980 *Phys. Rev.* A **22** 1615
[33] Fujikawa T 1983 *J. Phys. Soc. Japan* **52** 4001
[34] Vedrinskii R V, Bugaev L A, Gegusin I I, Kraizman V L, Novakovich A A, Prosandeev S A, Ruus R E, Maiste A A and Elango M A 1982 *Solid State Commun.* **44** 1401
[35] Lindner Th, Sauer H, Engel W and Kambe K 1986 *Phys. Rev.* B **33** 22
[36] Nakai S, Ohashi M, Ogata K, Yanagihara M and Maezawa H 1984 *Photon Factory Activity Report 1982/83* No. VI-73

[37] Van Vleck J H 1939 *J. Chem. Phys.* **7** 72
[38] Gerritsen H J and Lewis H R 1960 *Phys. Rev.* **119** 1010
[39] Caruthers E, Kleinman L and Zhang H I 1973 *Phys. Rev.* B **7** 3753
[40] Buffat B and Tuiller M H 1987 *Solid State Commun.* **64** 401
[41] Ulrici W 1984 *Modern Problems in Condensed Matter Sciences* vol 7 (Amsterdam: North-Holland)
Jahn H A and Teller E 1937 *Proc. R. Soc.* A **161** 220
[42] Liehr A D and Ballhausen C J 1958 *Ann. Phys., Lpz.* **3** 304
[43] McClure D S 1962 *J. Chem. Phys.* **36** 2757
[44] Koswig H D, Retter U and Ulrici W 1967 *Phys. Status Solidi* **24** 605